Research Article Vol. 30, No. 24 / 21 Nov 2022 / Optics Express 43480
Optics EXPRESS

Optical data transmission through highly dynamic and turbid water using dynamic scaling factors and single-pixel detector

ZILAN PAN,[1] YIN XIAO,[1] YONGGUI CAO,[1] LINA ZHOU,[1] AND WEN CHEN[1,2,*]

[1]Department of Electronic and Information Engineering, The Hong Kong Polytechnic University, Hong Kong, China
[2]Photonics Research Institute, The Hong Kong Polytechnic University, Hong Kong, China
*owen.chen@polyu.edu.hk

Abstract: Free-space optical data transmission through non-static scattering media, e.g., dynamic and turbid water, is challenging. In this paper, we propose a new method to realize high-fidelity and high-robustness free-space optical data transmission through highly dynamic and turbid water using a series of dynamic scaling factors to correct light intensities recorded by a single-pixel bucket detector. A fixed reference pattern is utilized to obtain the series of dynamic scaling factors during optical data transmission in free space. To verify the proposed method, different turbidity levels, different strengths of water-flow-induced turbulence and a laser with different wavelengths are studied in optical experiments. It is demonstrated that the proposed scheme is robust against water-flow-induced turbulence and turbid water, and high-fidelity free-space optical information transmission is realized at wavelengths of 658.0 nm and 520.0 nm. The proposed method could shed light on the development of high-fidelity and high-robustness free-space optical data transmission through highly dynamic and turbid water.

1. Introduction

Free-space optical communication is promising for versatile, secure and high-bandwidth data transmission in various applications, e.g., underwater [1–4]. Recently, there has been much research interest in using light as information carrier in underwater transmission links, since the light can provide the larger bandwidth, higher capacity, and lower power consumption compared to other communication techniques [5–9]. A challenging scenario is free-space optical data transmission through dynamic and turbid water, and it is well recognized that complex water environment could hinder applications of optical wireless communication. There is a severe power loss of optical wave in highly dynamic and turbid water environment, and the power loss is mainly due to absorption, scattering and turbulence [10–14]. Absorption and scattering depend on the wavelength of light and water properties, e.g., density and particles. The turbulence also imposes a limit on the propagating wave due to the fluctuation in refractive index of water in the presence of air bubbles, temperature and salinity [15–18], and could induce beam wandering and wavefront distortion. Until now, much research was focused on the enhancement of data rate and working distance [19–21] in free-space optical communication. However, real situations related to free-space optical data transmission in water environment, e.g., strong turbulence and dynamic water, may be overlooked in previous work. This issue is still open for research. In addition, much research work used a tank filled with clean water in optical experiments. However, in real water environments, attenuation coefficient is significantly high due to particles, air bubbles and turbulence. Therefore, it is desirable to develop new approaches to retrieving accurate signals, when optical wave propagates through highly dynamic and turbid water.

#474922 https://doi.org/10.1364/OE.474922
Journal © 2022 Received 5 Sep 2022; revised 27 Sep 2022; accepted 2 Oct 2022; published 10 Nov 2022

Optics EXPRESS

In this paper, a new approach is proposed to establish a high-fidelity and high-robustness optical wireless transmission channel through highly dynamic and turbid water using a series of dynamic scaling factors to correct light intensities recorded by a single-pixel bucket detector. To the best of our knowledge, this is the first investigation of utilizing dynamic scaling factors to realize high-fidelity and high-robustness free-space optical data transmission in highly dynamic and turbid water environment. A signal to be transmitted is considered as a series of independent pixels, and each pixel value is encoded into a 2D random amplitude-only pattern. The series of generated random amplitude-only patterns, called illumination patterns, is sequentially embedded into a spatial light modulator (SLM), and a fixed reference pattern, i.e., a pre-generated random amplitude-only pattern, is used before each illumination pattern to correct the recorded light intensities. Optical wave is diffused through highly dynamic and turbid water, and a single-pixel bucket detector [22–24] is used to record a series of light intensities. The proposed method is experimentally verified by using different turbid water conditions, different strengths of water-flow-induced turbulence and a laser with different wavelengths. Experimental results demonstrate that high-fidelity irregular analog signals can be retrieved by using the proposed method, and high robustness against turbulence generated by water flow is achieved.

2. Principle

A schematic experimental setup is shown in Fig. 1 to verify the developed free-space optical data transmission through highly dynamic and turbid water. In Fig. 1, a laser is controlled by using a laser diode mount (Thorlabs, LDM56/M) in a range of 0-500 mA, and three different wavelengths are individually used, i.e., 658.0 nm, 520.0 nm and 405.0 nm. A lens with focal length of 100.0 mm is utilized to collimate the laser beam, and then the collimated optical wave illuminates an amplitude-only SLM (Holoeye, LC-R720) with pixel size of 20.0 μm. The modulated optical wave propagates through highly dynamic and turbid water tank, and a stirrer is used to generate dynamic water environment. In this study, a water tank with size of 10.0 cm (L) × 25.0 cm (W) × 30.0 cm (H) is used to conduct a proof-of-principle experiment and verify the proposed method. The longer transmission distance can also be used in the proposed scheme, and the propagation distance through dynamic and turbid water could be estimated by using Beer-Lambert law. A single-pixel bucket detector (Newport, 918D-UV-OD3R) with optical power meter (Newport, 1936-R) is applied to record a series of light intensities at the receiving end. In optical experiments, axial distance between the SLM and water tank is 10.0 cm, and axial distance between water tank and single-pixel bucket detector is 5.0 cm.

In the developed free-space optical data transmission system, a signal to be transmitted is first encoded into a series of 2D random amplitude-only patterns to be sequentially embedded into the SLM in Fig. 1. The optical data encoding process is as follows:

(1) generate a 2D random matrix (512×512 pixels) with real and positive values;

(2) apply fast Fourier transform (FFT) to the 2D random matrix generated in Step (1) to obtain its spectrum;

(3) replace zero frequency of the generated spectrum in Step (2) by a pixel value of original signal, and then a new Fourier spectrum is obtained;

(4) apply inverse fast Fourier transform (IFFT) to the new Fourier spectrum obtained in Step (3) to generate an updated random amplitude-only pattern (P);

(5) repeat the above Steps (1)-(4) until every pixel of original signal is encoded into a 2D random amplitude-only pattern. The series of generated random amplitude-only patterns (P) can be sequentially embedded into the SLM in Fig. 1. Since it is impossible to use the SLM to directly display the generated pattern that contains negative values, a positive

Optics EXPRESS

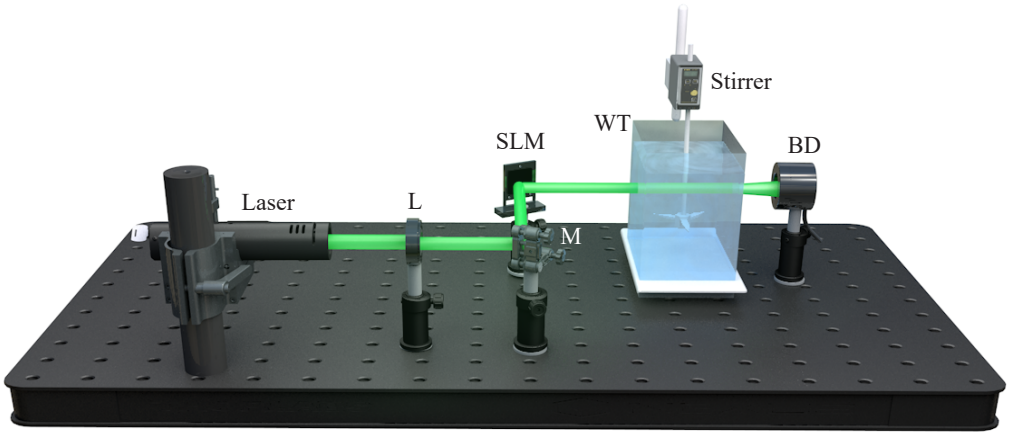

Fig. 1. A schematic experimental setup to verify the proposed method: L: Lens; M: Mirror; SLM: Amplitude-only spatial light modulator; WT: Turbid water tank; BD: Single-pixel bucket detector.

and real constant m is further used to divide each generated pattern (P) into two separate patterns ($m + P$) and (m-P), called illumination patterns.

In Fig. 1, the propagating wave is distorted by highly dynamic and turbid water, i.e., via scattering, absorption and turbulence. Attenuation coefficient $\mu(\lambda)$ consists of absorption and scattering which are related to wavelength of the laser, respectively denoted by $\mu_a(\lambda)$ and $\mu_s(\lambda)$. In the optical transmission through turbid water, absorption leads to a large power loss in the wave propagation path, and absorption coefficient depends on light wavelength and water properties (e.g., different chemical compositions of dissolved materials). Scattering deflects the photons in random directions, and leads to beam wandering and wavefront distortion. These attenuations [25–29] affect the light intensities recorded at the receiving end, and according to Beer-Lambert law [30–33] the process can be described by

$$I(d) = I_0 e^{-\mu(\lambda)d}, \tag{1}$$

$$\mu(\lambda) = \mu_a(\lambda) + \mu_s(\lambda), \tag{2}$$

where I_0 denotes incident light intensity, $I(d)$ denotes output light intensity, and d denotes the path length. In addition, the turbulence is also induced by random changes of refractive index in the wave propagation path due to salinity, temperature and pressure.

To obtain dynamic scaling factors in highly dynamic and turbid water environment, a fixed reference pattern $R(x,y)$, i.e., a random amplitude-only pattern, is further proposed here and embedded into the SLM before each illumination pattern, i.e., ($m + P$) and (m-P). At the receiving end, light intensities are recorded by using the single-pixel bucket detector in Fig. 1. The recording process is described by

$$\mathrm{B}_{ir} = k_i(t_i) \iint R(x,y)\, e^{-2\pi j(x\xi+y\eta)} dxdy|_{\xi=0,\eta=0} + noise, \tag{3}$$

$$\mathrm{B}_{i1} = k_i(t_{i+1}) \iint [m + P(x,y)]\, e^{-2\pi j(x\xi+y\eta)} dxdy|_{\xi=0,\eta=0} + noise, \tag{4}$$

$$\bar{\mathrm{B}}_{ir} = k_{i+1}(t_{i+2}) \iint R(x,y)\, e^{-2\pi j(x\xi+y\eta)} dxdy|_{\xi=0,\eta=0} + noise, \tag{5}$$

Optics EXPRESS

$$\mathrm{B}_{i2} = k_{i+1}(t_{i+3}) \iint [m - P(x,y)]\, e^{-2\pi j(x\xi+y\eta)} dxdy|_{\xi=0,\eta=0} + noise, \tag{6}$$

where $j = \sqrt{-1}$, (x,y) denotes coordinate in spatial domain, (ξ,η) denotes coordinate in frequency domain, B_{i1} and B_{i2} denote the recorded intensity values corresponding to the ith pixel of the transmitted signal, B_{ir} and $\bar{B}_{ir}$ denote the recorded intensity values corresponding to the reference pattern, and $k(t)$ denotes time-varying (dynamic) scaling factors. In the free-space optical data transmission system, environmental and shot noise is always induced. Since every time interval between the reference pattern and each illumination pattern (e.g., t_{i+1}-t_i or t_{i+3}-t_{i+2}) is short, adjacent scaling factors can be assumed to be the same, i.e., $k_i(t_i) \approx k_i(t_{i+1})$ and $k_{i+1}(t_{i+2}) \approx k_{i+1}(t_{i+3})$.

Therefore, each pixel value B_i of a signal obtained at the receiving end is retrieved by

$$\begin{aligned} B_i &= \frac{B_{i1}}{B_{ir}} - \frac{B_{i2}}{\bar{B}_{ir}} \\ &= \frac{k_i(t_{i+1}) \iint [m + P(x,y)]\, dxdy + noise}{k_i(t_i) \iint R(x,y)\, dxdy + noise} - \frac{k_{i+1}(t_{i+3}) \iint [m - P(x,y)]\, dxdy + noise}{k_{i+1}(t_{i+2}) \iint R(x,y)\, dxdy + noise} \\ &\approx \frac{1}{\iint R(x,y) dxdy + noise} \left\{ \iint [m + P(x,y)]\, dxdy - \iint [m - P(x,y)]\, dxdy \right\} \\ &= \frac{2}{\iint R(x,y)\, dxdy + noise} \iint P(x,y) dxdy \\ &\propto \iint P(x,y) dxdy \end{aligned} \tag{7}$$

It can be seen in Eq. (7) that noise can be effectively suppressed, and the retrieved intensity value is proportional to original signal pixel. Therefore, high-fidelity signals can be retrieved at the receiving end in the proposed free-space optical data transmission through highly dynamic and turbid water.

3. Experimental results and discussion

3.1. Turbidity

To verify the proposed method, different volumes of milk are mixed with clean water to be placed in the water tank in Fig. 1. Dissolving milk in clean water creates particle suspension, and can change attenuation coefficients. To emulate the turbidity, different volumes of milk are added to clean water with volume of 3.0 L, resulting in a variation of attenuation coefficients. Beer's coefficient $\mu(\lambda)$ is calculated based on Eq. (1), and is used to describe turbidity level [30,31] in this study. Performance of the developed free-space optical data transmission system through highly dynamic and turbid water can be evaluated, and experimental results are shown in Figs. 2 and 3.

To quantitatively evaluate quality of the signals retrieved at the receiving end, peak signal-to-noise ratio (PSNR) [32,33] is calculated. Figure 2 shows PSNR values of the retrieved signals, when turbidity of water in the tank, i.e., attenuation coefficient, is 3.24×10^{-2}, 3.60×10^{-2}, 3.68×10^{-2}, 3.74×10^{-2}, 3.84×10^{-2}, 3.91×10^{-2}, 3.97×10^{-2}, 4.11×10^{-2}, 4.12×10^{-2}, 4.13×10^{-2}, 4.14×10^{-2} and 4.16×10^{-2}, respectively. It can be seen in Fig. 2 that PSNR decreases with the increase of water turbidity level. When the turbidity is not larger than 3.97×10^{-2}, the retrieved signals are of high fidelity as shown in Figs. 3(a)–3(c). It is illustrated that the proposed method is feasible and effective. When attenuation coefficients are larger than 3.97×10^{-2}, PSNR values of the retrieved analog signals decrease dramatically as shown in Fig. 3(d). Due to the accumulation feature, scattering becomes stronger as milk concentration

Optics EXPRESS

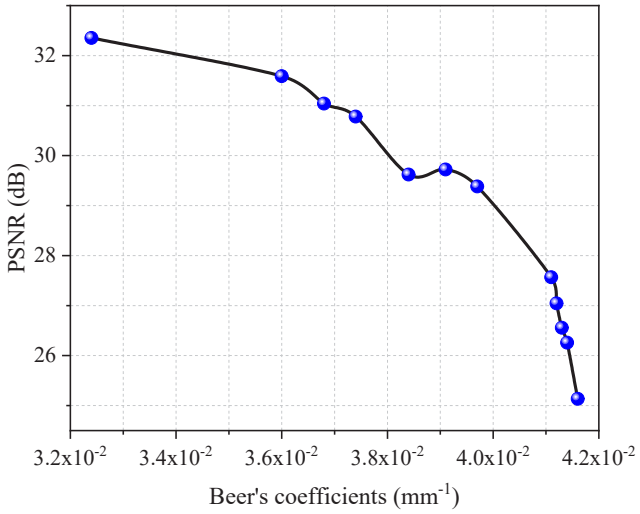

Fig. 2. PSNR values of the retrieved signals using the proposed method in the free-space optical data transmission through highly dynamic and turbid water when different water turbidities are used and tested. In this experiment, speed of the stirrer is 900.0 rpm.

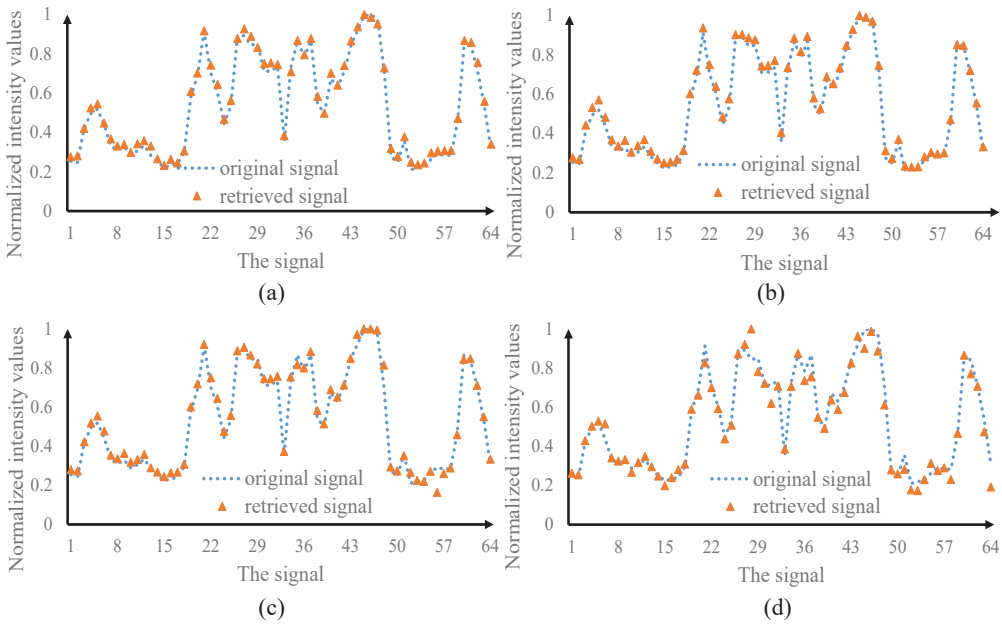

Fig. 3. Comparisons between original signal and the experimentally retrieved signals at the receiving end when different volumes of milk are used in the water tank to have an attenuation coefficient of (a) 3.24×10^{-2}, (b) 3.74×10^{-2}, (c) 3.97×10^{-2} and (d) 4.13×10^{-2}.

Optics EXPRESS

increases. It is also demonstrated in Figs. 2 and 3 that quality of the retrieved signals has a strong relationship with the detected light power, and highly dynamic and turbid water leads to a power loss of the propagating wave via scattering and absorption.

3.2. Water-flow-induced turbulence

A real water environment is always not static, and could be complex. A real water environment also produces turbulence. Therefore, we also investigate effect of water-flow-induced turbulence on the performance of the proposed method. In our study, dynamic water flow is generated by using a stirrer in Fig. 1, and different turbulence strengths are obtained by using different speeds of the stirrer in the water tank. The turbulences result in beam distortion and beam wandering, which cause large fluctuations of light intensities recorded at the receiving end.

In highly dynamic water environment, clean water and turbid water are respectively studied here. Turbid water is obtained by a mixture of clean water of 3.0 L and milk of 10.0 mL to be placed in the water tank in Fig. 1. The stirrer is used in optical experiments, and path loss and scintillation index are also calculated. The path loss is calculated by [34,35]

$$PL = 10 \times \log_{10}\left(\frac{P_t}{P_r}\right), \tag{8}$$

where PL denotes the loss (unit: dB), P_t denotes optical power just before water tank, and P_r denotes optical power collected by the single-pixel bucket detector. The optical power P_t just before water tank is 80.0 μW in our optical experiments. A relationship between speed of the stirrer and path loss is shown in Fig. 4. In addition, scintillation index is used and defined by [36,37]

$$\sigma_I^2 = \frac{\langle I^2 \rangle}{\langle I \rangle^2} - 1, \tag{9}$$

where $\langle \cdot \rangle$ denotes ensemble average, and I denotes the measured beam intensity by the single-pixel bucket detector at the receiving end. A relationship between speed of the stirrer and average scintillation index is shown in Fig. 5.

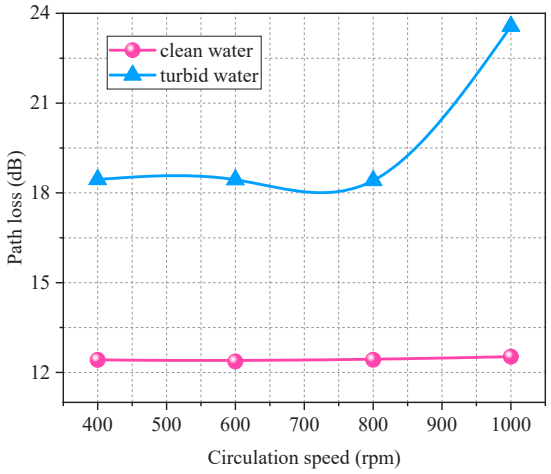

Fig. 4. Path loss due to wave propagation through clean water and turbid water in the tank when speed of the stirrer is 400.0, 600.0, 800.0 and 1000.0 rpm, respectively.

It can be seen in Fig. 4 that path loss in clean water is smaller than that in turbid water, and the path loss increases dramatically in turbid water environment when speed of the stirrer approaches

Optics EXPRESS

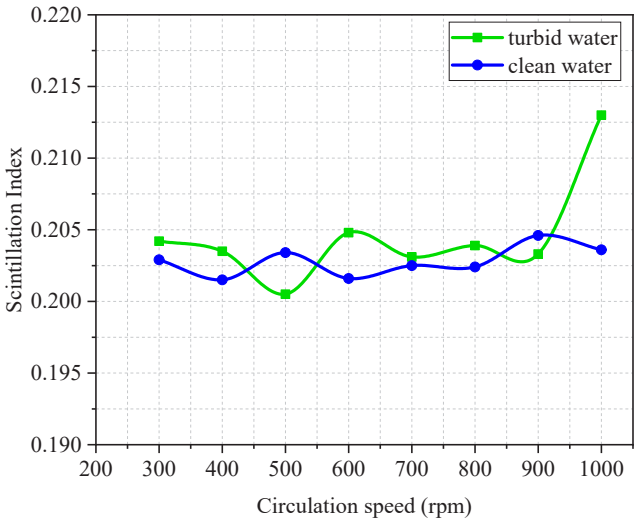

Fig. 5. A relationship between speed of the stirrer and average scintillation index obtained when clean water and turbid water are respectively used.

1000.0 rpm. It can be seen in Fig. 5 that the range of scintillation index is 0.201-0.205 in clean water and 0.200-0.213 in turbid water, which is larger than that used in other work [38].

The typically retrieved analog signals are shown in Figs. 6(a)–6(h). It is demonstrated that the retrieved signals are of high fidelity, and the proposed method is feasible and effective. When speed of the stirrer increases, PSNR values of the retrieved signals declines as shown in Fig. 7. When speed of the stirrer is not higher than 900.0 rmp, the retrieved signals are always of high quality as shown in Figs. 6(a)–6(f) and 7. It is also indicated that as velocity of dynamic scattering medium increases, there are severe and harsh turbulences. When water flow increases, particles in the water move rapidly which results in the larger power loss and wave distortion. It is verified that high-fidelity irregular analog signals can always be retrieved at the receiving end using the proposed method, and high robustness against highly dynamic and turbid water is achieved.

3.3. *Laser with different wavelengths*

The laser with different wavelengths, i.e., 405.0 nm blue laser (Thorlabs, DL5146-101S), 520.0 nm green laser (Thorlabs, L520P50) and 658.0 nm red laser (Thorlabs, L658P040), is individually used to further verify the proposed method. Turbid water is prepared by a mixture of clean water of 3.0 L and milk of 10.0 mL to be placed in water tank as shown in Fig. 1. Milk serves as a strongly scattering material, which has spheroidically-shaped particles floating in water. According to Mie scattering for spheroids, there is a linear downward trend on the percent of scattering light with an increment of the wavelength [39]. Therefore, light with the longer wavelength can propagate longer in turbid water. Figure 8 shows PSNR values of the retrieved signals, when different speeds of the stirrer and a laser beam with three different wavelengths are used. It can be seen in Fig. 8 that high-fidelity free-space optical information transmission is also realized by using the proposed method at wavelengths of 658.0 nm and 520.0 nm, and it is impossible to realize high-fidelity data transmission at wavelength of 405.0 nm. It is illustrated that a laser with long wavelengths (e.g., 658.0 nm and 520.0 nm) is feasible in the proposed method compared with short wavelength (e.g., 405.0 nm), when there is highly dynamic and turbid water in the wave propagation path.

Optics EXPRESS

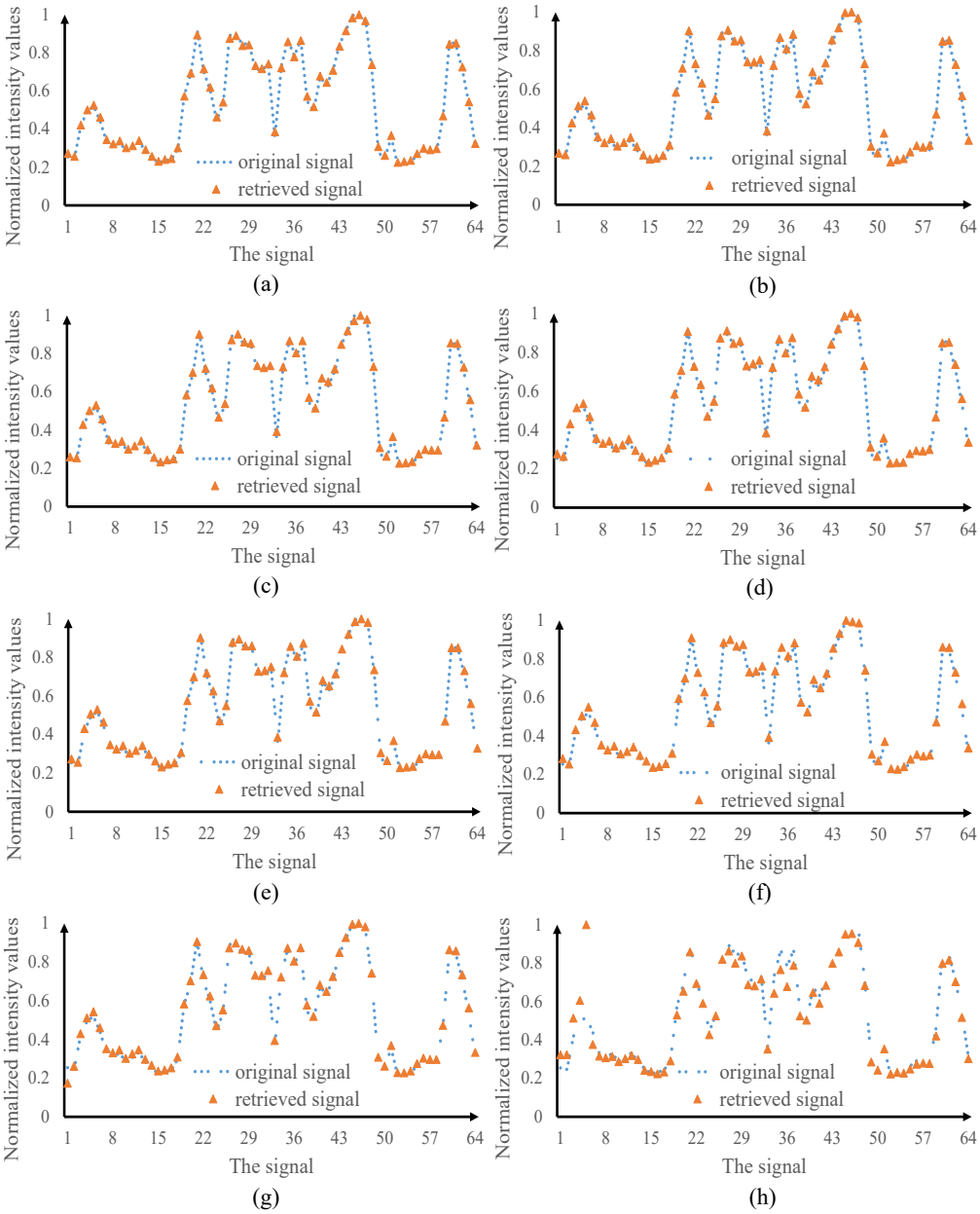

Fig. 6. (a)-(h) Comparisons between the retrieved analog signals at the receiving end and original signals respectively in clean water and turbid water when different speeds of the stirrer are used: i.e., (a), (b) 400 rpm; (c), (d) 600 rpm; (e), (f) 800 rpm; and (g), (h) 1000 rpm. (a), (c), (e) and (g) in clean water; (b), (d), (f) and (h) in turbid water.

Optics EXPRESS

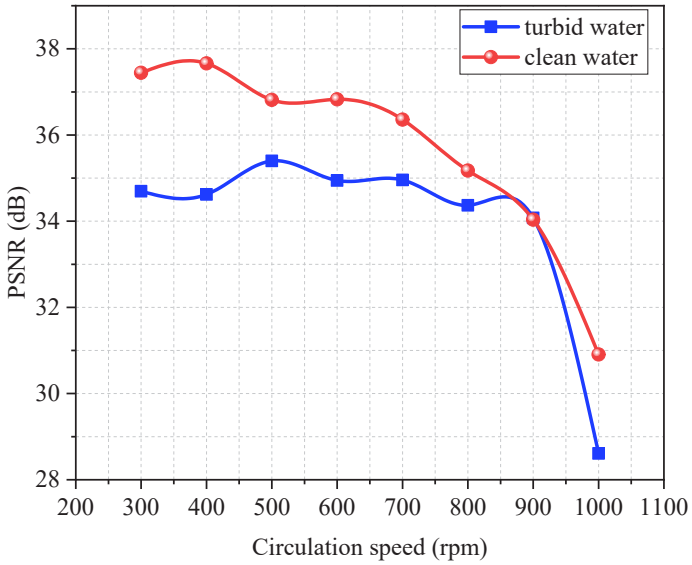

Fig. 7. A relationship between speed of the stirrer and quality of the retrieved signals.

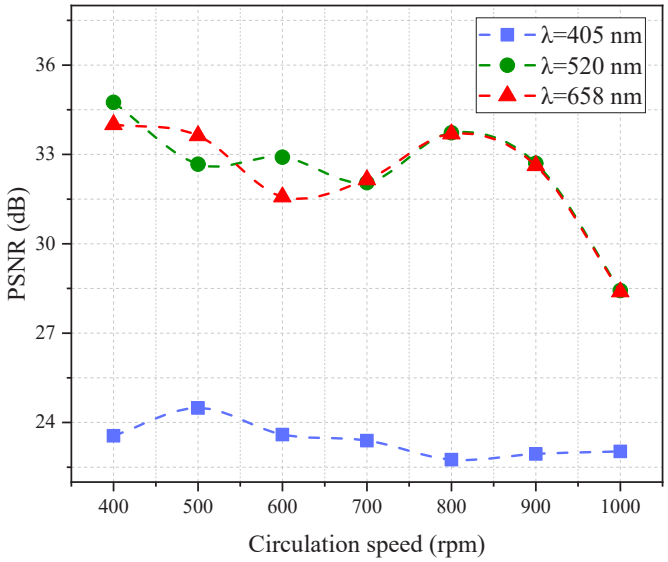

Fig. 8. PSNR values of the retrieved signals obtained when different speeds of the stirrer and a laser beam with three different wavelengths are respectively used. The irregular analog signal in Fig. 3 is tested.

Optics EXPRESS

4. Conclusion

We propose a new approach to establishing a high-fidelity and high-robustness optical wireless transmission channel through highly dynamic and turbid water using a series of dynamic scaling factors to correct the light intensities recorded by a single-pixel bucket detector. A series of generated 2D random amplitude-only patterns are sequentially embedded into the SLM, and a fixed reference pattern is used before each illumination pattern to correct the series of recorded light intensities. The optical wave is severely diffused through highly dynamic and turbid water, and a single-pixel bucket detector is used to record a series of light intensities. The proposed method is experimentally verified by using different turbid water conditions, different strengths of water-flow-induced turbulence and a laser with different wavelengths. It is demonstrated that high-fidelity irregular analog signals can always be retrieved at the receiving end using the proposed method, and high robustness against highly dynamic and turbid water is achieved. The proposed method could open up a novel research perspective for the development of high-fidelity and high-robustness free-space optical data transmission through highly dynamic and turbid water. It can be expected that the proposed method is feasible to realize optical data transmission in various environments, e.g., biological tissues, and around a corner [32,40–42].

Funding. Basic and Applied Basic Research Foundation of Guangdong Province (2022A1515011858); Hong Kong Research Grants Council (C5011-19G, 15224921, 15223522); The Hong Kong Polytechnic University (G-R006, 4-R006, 1-W167, 1-W19E, 1-BD4Q).

Disclosures. The authors declare no conflicts of interest.

Data availability. Data underlying the results presented in this paper are not publicly available at this time but may be obtained from the authors upon reasonable request.

References

1. M. A. Khalighi and M. Uysal, "Survey on free space optical communication: a communication theory perspective," IEEE Commun. Surv. Tutorials **16**(4), 2231–2258 (2014).
2. V. W. S. Chan, "Free-space optical communications," J. Lightwave Technol. **24**(12), 4750–4762 (2006).
3. A. K. Majumder and J. C. Ricklin, *Free-Space Laser Communications: Principles and Advances* (Springer, 2008), Chap.1.
4. G. Gibson, J. Courtial, M. J. Padgett, M. Vasnetsov, V. Pas'ko, S. M. Barnett, and S. Franke-Arnold, "Free space information transfer using light beams carrying orbital angular momentum," Opt. Express **12**(22), 5448–5456 (2004).
5. Z. Zeng, S. Fu, H. Zhang, Y. Dong, and J. Cheng, "A survey of underwater optical wireless communications," IEEE Commun. Surv. Tutorials **19**(1), 204–238 (2017).
6. C.-C. Kao, Y.-S. Lin, G.-D. Wu, and C.-J. Huang, "A comprehensive study on the internet of underwater things: applications, challenges, and channel models," Sensors **17**(7), 1477 (2017).
7. B. Cochenour, L. J. Mullen, and A. E. Laux, "Characterization of the beam-spread function for underwater wireless optical communications links," IEEE J. Oceanic Eng. **33**(4), 513–521 (2008).
8. M. Chitre, S. Shahabudeen, and M. Stojanovic, "Underwater acoustic communications and networking: recent advances and future challenges," Mar. Technol. Soc. J. **42**(1), 103–116 (2008).
9. D. O'Brien, G. E. Faulkner, E. B. Zyambo, K. Jim, D. J. Edwards, P. Stavrinou, G. Parry, J. Bellon, M. J. Sibley, V. A. Lalithambika, V. M. Joyner, R. J. Samsudin, D. M. Holburn, and R. J. Mears, "Integrated transceivers for optical wireless communication," IEEE J. Sel. Top. Quantum Electron. **11**(1), 173–183 (2005).
10. P. Sebbah, eds. *Waves and Imaging Through Complex Media* (Kluwer Academic, 2001).
11. D. S. Wiersma, "Disordered photonics," Nat. Photonics **7**(3), 188–196 (2013).
12. M. Kim, Y. Choi, C. Yoon, W. Choi, J. Kim, Q. H. Park, and W. Choi, "Maximal energy transport through disordered media with the implementation of transmission eigenchannels," Nat. Photonics **6**(9), 581–585 (2012).
13. Y. Weng, Y. Guo, O. Alkhazragi, T. K. Ng, J.-H. Guo, and B. S. Ooi, "Impact of turbulent-flow-induced scintillation on deep-ocean wireless optical communication," J. Lightwave Technol. **37**(19), 5083–5090 (2019).
14. H. Kaushal and G. Kaddoum, "Underwater optical wireless communication," IEEE Access **4**, 1518–1547 (2016).
15. H. M. Oubei, E. Zedini, R. T. ElAfandy, A. Kammoun, M. Abdallah, T. K. Ng, M. Hamdi, M.-S. Alouini, and B. S. Ooi, "Simple statistical channel model for weak temperature-induced turbulence in underwater wireless optical communication systems," Opt. Lett. **42**(13), 2455–2458 (2017).
16. P. Qiu, G. Cui, Z. Qian, S. Zhu, X. Shan, Z. Zhao, X. Zhou, X. Cui, and P. Tian, "4.0 Gbps visible light communication in a foggy environment based on a blue laser diode," Opt. Express **29**(9), 14163–14173 (2021).
17. Y. Zhao, A. Zhao, L. Zhu, W. Lv, J. Xu, S. Li, and J. Wang, "Performance evaluation of underwater optical communications using spatial modes subjected to bubbles and obstructions," Opt. Lett. **42**(22), 4699–4702 (2017).

Optics EXPRESS

18. M. V. Jamali, A. Mirani, A. Parsay, B. Abolhassani, P. Nabavi, A. Chizari, P. Khorramshahi, S. Abdollahramezani, and J. A. Salehi, "Statistical studies of fading in underwater wireless optical channels in the presence of air bubble, temperature, and salinity random variations," IEEE Trans. Commun. **66**(10), 4706–4723 (2018).
19. X. Yang, Z. Tong, Y. Dai, X. Chen, H. Zhang, H. Zou, and J. Xu, "100 m full-duplex underwater wireless optical communication based on blue and green lasers and high sensitivity detectors," Opt. Commun. **498**, 127261 (2021).
20. C. H. Kang, A. Trichili, O. Alkhazragi, H. Zhang, R. C. Subedi, Y. Guo, S. Mitra, C. Shen, I. S. Roqan, N. G. Tien Khee, M.-S. Alouini, and B. S. Ooi, "Ultraviolet-to-blue color-converting scintillating-fibers photoreceiver for 375-nm laser-based underwater wireless optical communication," Opt. Express **27**(21), 30450–30461 (2019).
21. J. Wang, C. Lu, S. Li, and Z. Xu, "100 m/500 Mbps underwater optical wireless communication using an NRZ-OOK modulated 520 nm laser diode," Opt. Express **27**(9), 12171–12181 (2019).
22. E. Tajahuerce, V. Durán, P. Clemente, E. Irles, F. Soldevila, P. Andrés, and J. Lancis, "Image transmission through dynamic scattering media by single-pixel photodetection," Opt. Express **22**(14), 16945–16955 (2014).
23. K. Soltanlou and H. Latifi, "Three-dimensional imaging through scattering media using a single pixel detector," Appl. Opt. **58**(28), 7716–7726 (2019).
24. Y. Xiao, L. Zhou, and W. Chen, "Experimental demonstration of ghost-imaging-based authentication in scattering media," Opt. Express **27**(15), 20558–20566 (2019).
25. N. Enghiyad and A. G. Sabbagh, "Impulse response of underwater optical wireless channel in the presence of turbulence, absorption, and scattering employing Monte Carlo simulation," J. Opt. Soc. Am. A **39**(1), 115–126 (2022).
26. L. Lu, X. Ji, and Y. Baykal, "Wave structure function and spatial coherence radius of plane and spherical waves propagating through oceanic turbulence," Opt. Express **22**(22), 27112–27122 (2014).
27. L. Lu, P. Zhang, C. Fan, and C. Qiao, "Influence of oceanic turbulence on propagation of a radial Gaussian beam array," Opt. Express **23**(3), 2827–2836 (2015).
28. H. Song, R. Zhang, N. Hu, H. Zhou, X. Su, H. Song, K. Zou, K. Pang, C. Liu, D. Park, B. Lynn, G. Gbur, A. Dogariu, R. Watkins, J. Miller, E. Johnson, M. Tur, and A. Willner, "Dynamic aerosol and dynamic air-water interface curvature effects on a 2-Gbit/s free-space optical link using orbital-angular-momentum multiplexing," Nanophotonics **11**(4), 885–895 (2022).
29. Z. Y. Zhu, M. Janasik, A. Fyffe, H. Darrick, Y. Y. Zhou, B. Kantor, T. Winder, R. W. Boyd, G. Leuchs, and Z. M. Shi, "Compensation-free high- dimensional free-space optical communication using turbulence-resilient vector beams," Nat. Commun. **12**(1), 1–8 (2021).
30. S. Komatsu, A. Markman, and B. Javidi, "Optical sensing and detection in turbid water using multidimensional integral imaging," Opt. Lett. **43**(14), 3261–3264 (2018).
31. R. Joshi, G. Krishnan, T. O'Connor, and B. Javidi, "Signal detection in turbid water using temporally encoded polarimetric integral imaging," Opt. Express **28**(24), 36033–36045 (2020).
32. Z. Pan, Y. Xiao, L. Zhou, Y. Cao, M. Yang, and W. Chen, "Non-line-of-sight optical information transmission through turbid water," Opt. Express **29**(24), 39498–39510 (2021).
33. Z. Pan, Y. Xiao, Y. Cao, L. Zhou, and W. Chen, "Optical analog-signal transmission and retrieval through turbid water," Appl. Opt. **60**(34), 10704–10713 (2021).
34. S. Tang, Y. Dong, and X. Zhang, "On path loss of NLOS underwater wireless optical communication links," in *Proceedings of IEEE Conference on Oceans, IEEE Xplore*, 1–3 (2013).
35. Y. Zuo, H. Xiao, J. Wu, Y. Li, and J. Lin, "A single-scatter path loss model for non-line-of-sight ultraviolet channels," Opt. Express **20**(9), 10359–10369 (2012).
36. L. C. Andrews, R. L. Phillips, and C. Y. Hopen, *Laser Beam Scintillation with Applications* (SPIE, 2001).
37. Y. Gu, O. Korotkova, and G. Gbur, "Scintillation of nonuniformly polarized beams in atmospheric turbulence," Opt. Lett. **34**(15), 2261–2263 (2009).
38. Y. Guo, M. Kong, M. Sait, S. Marie, O. Alkhazragi, T. K. Ng, and B. S. Ooi, "Compact scintillating-fiber/450-nm-laser transceiver for full-duplex underwater wireless optical communication system under turbulence," Opt. Express **30**(1), 53–69 (2022).
39. T. M. P. Cattaneo and S. E. Holroyd, "The use of near infrared spectroscopy for determination of adulteration and contamination in milk and milk powder: updating knowledge," J. Near Infrared Spectrosc. **21**(5), 341–349 (2013).
40. Z. Pan, Y. Xiao, Y. Cao, L. Zhou, and W. Chen, "Accurate optical information transmission through thick tissues using zero-frequency modulation and single-pixel detection," Opt. Lasers Eng. **158**, 107133 (2022).
41. Y. Xiao and W. Chen, "High-fidelity optical transmission around the corner," IEEE Photon. Technol. Lett. **33**(1), 3–6 (2021).
42. Y. Cao, Y. Xiao, Z. Pan, L. Zhou, and W. Chen, "High-fidelity temporally-corrected transmission through dynamic smoke via pixel-to-plane data encoding," Opt. Express **30**(20), 36464–36477 (2022).